1-1-2013

CD2AP links cortactin and capping protein at the cell periphery to facilitate formation of lamellipodia

Jianping Zhao

Serawit Bruck

Saso Cemerski

Lei Zhang

Boyd Butler

See next page for additional authors

Authors

Jianping Zhao, Serawit Bruck, Saso Cemerski, Lei Zhang, Boyd Butler, Adish Dani, John A. Cooper, and Andrey S. Shaw

CD2AP Links Cortactin and Capping Protein at the Cell Periphery To Facilitate Formation of Lamellipodia

Jianping Zhao, Serawit Bruck, Saso Cemerski, Lei Zhang, Boyd Butler, Adish Dani, John A. Cooper and Andrey S. Shaw

---

Updated information and services can be found at:
http://mcb.asm.org/content/33/1/38

These include:

SUPPLEMENTAL MATERIAL   Supplemental material

REFERENCES   This article cites 48 articles, 17 of which can be accessed free at: http://mcb.asm.org/content/33/1/38#ref-list-1

CONTENT ALERTS   Receive: RSS Feeds, eTOCs, free email alerts (when new articles cite this article), more»

CD2AP Links Cortactin and Capping Protein at the Cell Periphery To Facilitate Formation of Lamellipodia

Jianping Zhao,[a] Serawit Bruck,[a]* Saso Cemerski,[a] Lei Zhang,[a] Boyd Butler,[b] Adish Dani,[a] John A. Cooper,[b] Andrey S. Shaw[a,c]

Department of Pathology and Immunology,[a] Department of Cell Biology and Physiology,[b] and Howard Hughes Medical Institute,[c] Washington University School of Medicine, St. Louis, Missouri, USA

Understanding the physiology of complex relationships between components of signaling pathways and the actin cytoskeleton is an important challenge. CD2AP is a membrane scaffold protein implicated in a variety of physiological and disease processes. The physiological function of CD2AP is unclear, but its biochemical interactions suggest that it has a role in dynamic actin assembly. Here, we report that CD2AP functions to facilitate the recruitment of actin capping protein (CP) to the Src kinase substrate, cortactin, at the cell periphery, and that this is necessary for formation of the short branched filaments that characterize lamellipodium formation and are required for cell migration. Superresolution fluorescence microscopy demonstrated that the efficient colocalization of CP and cortactin at the cell periphery required CD2AP. As both cortactin and CP function to enhance branched actin filament formation, CD2AP functions synergistically to enhance the function of both proteins. Our data demonstrate how the interplay between specialized actin regulatory molecules shapes the actin cytoskeleton.

Animal cells control their shape and move about by regulating the assembly of actin filaments in space and time. Unique cell shapes and movements are defining features of differentiated cell function, and they change in the course of pathological processes. While a number of molecular components capable of interacting with actin and controlling its polymerization have been identified, the field has a very limited understanding of how this complex array of components, with a multitude of biochemical interactions, works together to assemble actin and produce the forces that dictate shape and power movement.

Using biochemical approaches, we identified several actin regulatory proteins as interacting with the membrane scaffold CD2AP (1). However, the physiological significance of these interactions is not known. Here, we address this question with experiments that reveal that interactions of CD2AP with CP and cortactin indeed have physiological significance, and we elucidate how these interactions lead to spatial and temporal recruitment and assembly of the actin filament network that drives cell shape changes at the periphery of motile cells.

CD2AP is a signaling scaffold protein originally discovered to be necessary for the formation of the actin-based immunological synapse (2). CD2AP is expressed in a wide variety of cells, with higher levels in epithelial cells, immune cells, and neurons (3). Loss of CD2AP from glomerular epithelial cells, also known as podocytes, leads to renal failure (4). Human genetic studies have also implicated CD2AP in the pathogenesis of Alzheimer's disease (5, 6). Several groups, including our own, identified a biochemical interaction between CD2AP and CP (1, 7). In our previous work, we found the interaction between CP and CD2AP to be of high affinity (dissociation constant [K_d], 2.4 nM) (1), and we defined a CP binding motif in CD2AP which is present in a number of known CP binding proteins that are otherwise unrelated (8). Whether CD2AP binding to CP in cells enhances or inhibits the actin capping activity of CP remains an open question, along with the possibility that CD2AP recruits CP to the membrane. CD2AP was also found to associate with the actin regulatory protein cortactin in biochemical studies (9). Cortactin binds to F-actin and

the Arp2/3 complex, and this promotes the formation of branched networks of actin filaments (10–12). CD2AP interacts with the Src homology 3 (SH3) domain of cortactin, and epidermal growth factor induces formation of a CD2AP/cortactin complex in membrane ruffles (9). The physiological significance of this interaction, however, remains unclear.

Here, we examined, for the first time, the biological role of the CD2AP-CP interaction. We discovered that CD2AP recruits CP to the cell periphery, close to the actin filament barbed ends that can be capped by CP. Loss of CD2AP led to loss of CP recruitment to the cell periphery, and this depended on the direct interaction between the two proteins. Furthermore, we discovered that recruitment of CD2AP to the cell periphery was mediated by an interaction of CD2AP with cortactin. Together, our results suggest that the formation of lamellipodia is mediated by a complex of cortactin, CD2AP, and CP. The formation of this complex may help to create a feedback loop that promotes the formation of a branching network of actin filaments in lamellipodia.

MATERIALS AND METHODS

DNA constructs, lentivirus, and regents. Green fluorescent protein (GFP) fused to actin was subcloned into a retroviral expression vector driven by the pMX promoter (13). CD2AP short interfering RNA (siRNA) oligonucleotides were designed using Invitrogen BLOCK-iT

RNA interference (RNAi) design tools. The oligonucleotides were cloned into the pFLRu lentivirus vector with yellow fluorescent protein (YFP) tag provided by Greg Longmore (Washington University, St. Louis, MO) (14). The mutated forms of CD2AP were generated using PCR, cloned into pEGFP-C1/N1 vectors (Clontech), and confirmed by DNA sequencing. Mouse cortactin, RNAi-resistant cortactinR, and cortactinR-W525K (with a defective SH3 domain) (15) were cloned into pFLAG-CMV-6c (Sigma) or pTurboRFP-C vector (Evrogen). pFLRu-CD2AP-CT lentivirus vector was made by replacing YFP with GFP-CD2AP-CT (C-terminal half of CD2AP) in the pFLRu vector, and small hairpin RNAs (shRNAs) against cortactin (15) or luciferase were cloned into pFLRu-CD2AP-CT. Anti-CD2AP rabbit polyclonal antibody (Ab) was prepared in the laboratory. Anticortactin (MAb 4F11) was purchased from Millipore. Anti-FLAG (monoclonal Ab [MAb] M2) and agarose beads conjugated with anti-FLAG were from Sigma. Anti-GFP (MAb JL-8) was from Clontech, and anti-GFP (chicken IgY) was from Invitrogen.

Cell culture and transfection. Immortalized mouse podocytes derived from wild-type or CD2AP-deficient mice were cultured at 33°C in RPMI 1640 supplemented with antibiotics, 10% fetal calf serum, and gamma interferon (IFN-γ) (16). 293T cells were cultured in Dulbecco's modified Eagle medium (DMEM) supplemented with antibiotics and 10% fetal calf serum. Enhanced GFP (EGFP) fused to actin in a retroviral vector was transfected into Plat-E packaging cells (17). The virus secreted by these cells was used to infect the podocytes. Cells stably expressing low levels of GFP-actin were used for fluorescence recovery after photobleaching (FRAP) experiments, and a total internal reflection fluorescence (TIRF) microscope was used. CD2AP or cortactin RNAi lentivirus was used to infect podocytes, and RNAi efficiency was evaluated by Western blotting. Wild-type and CD2AP-deficient podocytes were transiently transfected with plasmids using Amaxa nucleofection (Lonza) or Lipofectamine 2000 (Invitrogen).

Cell motility, cell spreading, and video microscopy. Podocytes were grown in 60-mm tissue culture dishes to confluence, and a scratch wound was created with a pipette tip. Cells were allowed to recover for 30 min before imaging migration over a 24-h time period using bright-field optics on an upright microscope with a 10× objective. For video microscopy, a Cascade charge-coupled device (CCD) camera was used. Video was compiled using Metamorph software (Universal Imaging Corp). Alternatively, cells were stained with DRAQ5 (Alexis Biochemicals, Lausen, Switzerland) at time zero, and then, 17.5 h postscratch, they were fixed and imaged using a Zeiss LSM510 confocal microscope with a 10× objective. The number of cells that migrated toward the wound was counted for each cell type. Cell spreading was performed by replating trypsinized cells in Ringers lactate (5 mM HEPES, pH 7.2 to 7.4, 155 mM NaCl, 3 mM HCl, 2 mM $CaCl_2$, 1 mM $MgCl_2$, 3 mM NaH_2PO_4, 10 mM glucose) onto acid-washed coverslips. Cells were allowed to attach for 5 min and spread for 5 or 15 min. They were then fixed and imaged by phase-contrast microscopy.

TIRF microscopy. To image by TIRF the actin dynamics of spreading wild-type and CD2AP-deficient podocytes, we dropped trypsinized cells stably expressing GFP-actin on collagen-coated glass-bottom culture dishes (MatTek Corporation, Ashland, MA). The TIRF microscopy system (through the lens) included an inverted microscope (IX-81; Olympus America, Center Valley, PA) and an electron multiplication back-thinned frame transfer CCD video camera (model C9100-12; Hamamatsu Photonics, Bridgewater, NJ) with a 60×, 1.45-numerical-aperture (NA) PlanApo oil objective. SlideBook software (Intelligent Imaging Innovations, Denver, CO) operated the system and collected the images. Frames were collected every 3 s for 7 min.

Confocal microscopy, FRAP, and lamellipodium localization quantification. Cells were grown on acid-washed, 2.5-cm coverslips or glass dishes for 16 h before imaging. All live-cell imaging was performed at 37°C using a directly heated coverslip system (Bioptechs, Scranton, PA). Scanning confocal microscopy was performed on a Zeiss LSM 510 with a 40×, 1.2-NA water objective or Olympus FluoView FV1000. For the dynamics of actin in the cytoplasm or plasma membrane, GFP was bleached with 100% of an 8-mW, 488-nm laser applied to a 4- by 0.5-μm rectangle. This region was bleached for <5 s, and then the same region was imaged at less than 5% of the bleach power. The images were acquired at 200-ms intervals. The intensity of GFP-actin before bleaching was set at 1, and the bleaching was set at 0. The ratio of the recovered to the original intensity was plotted against time (in seconds) using Microsoft Excel. The intensity of the bleached area was corrected for photobleaching. The nonlinear fit analysis was conducted using PRISM5 software (Graphpad). To quantify lamellipodium localization, cells transfected with GFP-tagged CD2AP mutants were replated onto a glass coverslip and fixed with 4% paraformaldehyde (PFA). Using confocal microscopy, lamellipodia were identified as thin protrusive sheets of membrane at the periphery of the cell. As it is sometimes difficult to distinguish between membrane ruffles and lamellipodia, only cells exhibiting GFP signals in clearly discernible lamellipodia were counted as positive. For each group, averages of 80 to 100 cells were analyzed and quantified.

Immunoprecipitation. 293T cells were cotransfected with FLAG-cortactin and CD2AP or CD2AP-ΔPR2-GFP. Two days after transfection, the cells were lysed with phosphate-buffered saline (PBS) containing 1% Triton X-100, 10 mM NaF, 1 mM Na_3VO_4, 0.2 mM phenylmethylsulfonyl fluoride (PMSF), 1 μM pepstatin, 1 μg/ml aprotinin, and 10 μM leupeptin. The cell lysates (500 μg) were incubated with agarose beads conjugated with anti-FLAG MAb M2 (Sigma) at 4°C for 4 h. The beads were washed 5 times with 1% Triton X-100 in PBS, and immunoprecipitates were analyzed by immunoblotting with anti-GFP and anti-FLAG Abs.

STORM imaging. The stochastic optical reconstruction microscopy (STORM) setup and imaging were similar to those described before (18). Briefly, the STORM microscope was constructed around a Nikon Ti-E inverted microscope operating in wide-field epifluorescence mode and using the Nikon Perfect Focus system for focus stabilization. The activation/imaging lasers (CUBE 405 nm-50, Sapphire 561 nm-150, and Sapphire 460 nm-10 from Coherent and Stradus 642 nm-110 from Vortran Laser) were individually shuttered by a mechanical shutter (Uniblitz LS3ZM2; Vincent Associates) and an acousto-optical tunable filter (AOTF; PCAOM; Crystal Technology). Laser lines were combined, expanded, and collimated before being focused at the back focal plane of a 100× objective (100× UPlanSApo; NA, 1.4; Olympus). A quad-band dichroic mirror (zt405/488/561/640rpc; Chroma) and a band-pass filter (ET705/70m; Chroma) separated the fluorescence signal collected by the same objective from the excitation light. Images were recorded with an electron-multiplying CCD (EMCCD) camera (iXon Plus DU897; Andor).

Podocytes transfected with GFP-CP were plated on coverglass and stained with anti-CD2AP and anticortactin or anti-CD2AP and anti-GFP. Secondary antibodies for STORM were custom conjugated with Cy3-Alexa 647 (A647) and Alexa 405-A647 dye pairs as described before (6). Antibody control was prepared by adhering a diluted mixture of anti-mouse Cy3-A647-conjugated and anti-rabbit 405-A647-conjugated secondary antibodies to a coverglass flow cell. All imagings were performed by inverting coverslips onto a glass slide with imaging buffer (80:10:10:1 ratio of PBS, 1 M mercaptoethylamine [pH 8.5], 50% glucose solution in water, and an antibleaching oxygen scavenger system [10 mg of glucose oxidase plus 25 μl of catalase and 100 μl of PBS]). Excess buffer was drained and the edges sealed with nail polish before image acquisition.

Colocalization and cross-correlation analysis. STORM images of entire cells were reconstructed using Gaussian fitting to find the center position of single molecules. The fitted positions were saved as a binary image of localization/no localization with a pixilation grid size of 40 nm. Cross-correlation analysis was performed as described recently (19) on 6-μm² square regions of interest (ROI), using 10 ROIs for each cell and 6 cells for each sample. Cross-correlation functions of the ROI from two channels were calculated using a custom-written MatLab script using a fast Fourier transform (FFT). The cross-correlation function represents the probability of finding a second channel localization at a certain dis-
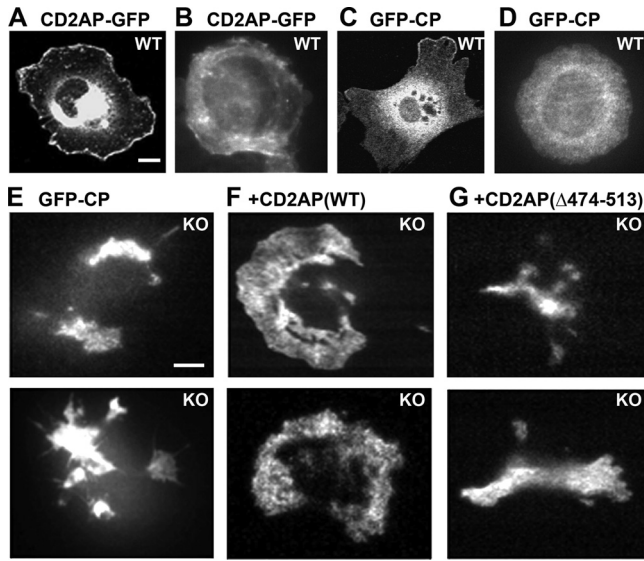
FIG 1 CD2AP facilitates CP recruitment to the cell periphery. Shown are a confocal image (A) and TIRF image (B) of a wild-type (WT) podocyte transiently transfected with CD2AP-GFP spreading on glass. Bar, 10 μm. (C and D) Confocal image (C) and TIRF image (D) of a wild-type podocyte transiently transfected with GFP-CP spreading on glass. (E) Defective CP recruitment to the cell periphery in CD2AP-deficient (KO) podocytes. CD2AP KO podocytes were transiently transfected with GFP-CP, plated on glass, and imaged using TIRF microscopy. Bar, 10 μm. (F) Expression of wild-type CD2AP rescues CP recruitment to the periphery during cell spreading. CD2AP KO podocytes were transiently cotransfected with wild-type CD2AP and GFP-CP and imaged using TIRF microscopy. The transfected cells were identified using immunofluorescence. (G) A mutated form of CD2AP (Δ474-513) unable to bind to CP cannot rescue the CP recruitment defect. CD2AP-deficient podocytes were transiently cotransfected with CD2AP (Δ474-513) and GFP-CP and then imaged by TIRF microscopy. We confirmed that the level of expression of the mutated CD2AP was similar to or higher than that of the wild-type CD2AP in individual cells by immunofluorescence staining with an antibody to CD2AP (data not shown).

tance, r, from the first channel. A value of 1 represents a random distribution between the two channels, and values higher than 1 suggest a correlation of two channel molecules at a certain distance.

Colocalization analysis was performed using Manders' overlap coefficient, which is based on Pearson's coefficient (20). Briefly, the Manders' overlap coefficient represents the degree of colocalization between the two channels. Ten randomly selected 6-μm² ROIs at the cell periphery and in cytoplasm in 6 separate cells were analyzed for each cell type. Six randomly selected 6-μm² regions of interest were also analyzed on the antibody control sample.

RESULTS

CP recruitment to the cell leading edge is impaired in CD2AP-deficient cells. Since CP is important in the formation of actin-based structures at the cell periphery (21, 22), our initial experiments examined whether CD2AP plays a role in CP recruitment to the periphery of spreading podocyte cells. Using both confocal and TIRF microscopy, we localized CD2AP and CP during the initial phases of cell spreading. We first confirmed that CD2AP is efficiently recruited to the cell periphery by expressing a green fluorescent protein (GFP)/CD2AP fusion protein (CD2AP-GFP). Wild-type podocytes were allowed to adhere to glass and spread for up to 30 min. Confocal microscopy showed that CD2AP was recruited to the cell periphery in ~56% of cells (Fig. 1A), and TIRF microscopy showed that it was evenly distributed on the adherent

surface of the cell during the process of cell spreading (Fig. 1B). The recruitment of CP to the periphery of wild-type podocytes was assessed using a GFP-capping protein fusion protein (GFP-CP). Confocal microscopy showed that it localized mainly in the cytoplasm and also at the periphery of the cell in a smooth and even pattern in ~43% of cells (Fig. 1C). TIRF microscopy showed that CP was recruited to the entire adherent surface of the cell (Fig. 1D).

To determine whether CP recruitment to the periphery was defective in CD2AP-deficient cells, we expressed GFP-CP in CD2AP-deficient podocytes and imaged its localization during spreading. In contrast to the wild-type cells, CP recruitment to the periphery was extremely irregular and patchy in CD2AP-deficient cells (Fig. 1E). This pattern was observed at early time points; at later time points (>60 min), the pattern resembled that seen in wild-type cells (data not shown). Thus, efficient recruitment of CP to the cell periphery at early time points during cell spreading might be mediated by CD2AP.

To confirm that the CP recruitment defect was due to the failure of CP to interact with CD2AP, we tested the function of a CD2AP mutant defective in binding CP. Expression of wild-type CD2AP in CD2AP-deficient podocytes largely rescued CP recruitment relative to the recruitment in the CD2AP-knockout cells as assessed by confocal and TIRF microscopy (Fig. 1F). Expression of a mutated form of CD2AP (Δ474-513), which lacks the CP binding site (1), was unable to rescue the peripheral recruitment of CP, and the cells were largely indistinguishable from CD2AP-deficient cells (Fig. 1G). Lastly, since Arg 493 and Lys 495 of CD2AP are both critical for the CP interaction, we generated a mutated form of CD2AP substituting alanine for both of these residues. As expected, the R493A/K495A mutant also failed to rescue the CP recruitment and spreading phenotype (data not shown). Thus, CD2AP facilitates the recruitment of CP to the periphery of spreading cells, apparently through a direct molecular interaction.

CD2AP influences the actin-based morphology of cell edges during podocyte spreading. Since CP is important in the formation of actin-based structures during cell spreading, we assessed the morphology of CD2AP-deficient cells during cell spreading by phase-contrast microscopy (Fig. 2A and B). As illustrated in Fig. 2A, we scored the morphology of spreading cells into three categories, smooth edged, filopodial, and ruffling, using a classification scheme developed by Borisy and coworkers (23). Wild-type cells generally exhibited either a circular spreading pattern with a flat, smooth edge (~35% at 5 min, ~60% at 15 min), which we would describe as lamellar, or they exhibited dynamic phase-dense, thick undulations, which were scored as ruffling (~45% at 5 min, 35% at 15 min) (Fig. 2B). CD2AP-deficient cells spread in an asymmetric pattern with an increased number of cells exhibiting dynamic finger-like projections of the cell edge (~20% at 5 min, 15% at 15 min), a pattern which we scored as filopodial with an increased number of cells exhibiting the ruffling appearance (70% at 5 min, 80% at 15 min) (Fig. 2B). Thus, cell spreading is affected by the loss of CD2AP, with changes in the morphology of the actin-based structures at the spreading edge of the cells. Interestingly, the observed increase in ruffling and filopodial patterns is similar to the effects described for the loss of CP (21, 22).

To examine the actin cytoskeleton during cell spreading, we expressed GFP-actin in the cells and used TIRF video microscopy. While wild-type cells exhibited a smooth and circumferential distribution of actin during spreading, the CD2AP-deficient cells ex-
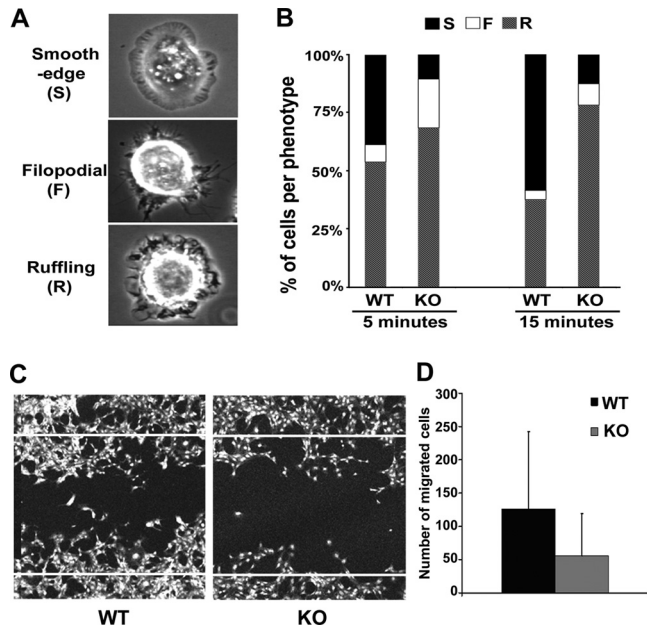
FIG 2 CD2AP is required for efficient cell spreading and migration. (A) Wild-type and CD2AP-deficient podocytes were plated onto glass coverslips and fixed after 5 or 15 min. Cells were classified into three different morphologies, examples of which are shown in Fig. 1. The smooth-edge phenotype is characterized by a flat, evenly spreading leading edge. The ruffling phenotype is characterized by phase-dense undulations of the peripheral membrane. The filopodial phenotype is characterized by finger-like protrusions at the periphery of the cell. (B) Quantification of the smooth-edge, ruffling, and filopodial phenotypes of wild-type and CD2AP-deficient podocytes. Phenotypes were assessed by phase-contrast microscopy of fixed podocytes at 5 and 15 min after making contact with a glass slide. Images were scored blinded and classified as one of the three phenotypes. Most of the wild-type podocytes displayed smooth-edge and ruffling phenotypes. In contrast, the CD2AP-deficient podocytes had a higher propensity to spread with ruffling phenotype. (C) Wound healing assay. Wild-type (WT) and CD2AP-deficient (KO) podocytes were grown to confluence. A wound was inflicted with a p200 pipette tip. At 17.5 h later, the cells were fixed and stained with DRAQ5 and imaged using confocal microscopy. The white lines represent the boundaries of the original wound. (D) Column bar graph showing the number of cells that migrated toward the wound. A box was drawn at the boundaries of the original wound, and cells within the box after 17.5 h were counted. Fewer CD2AP-deficient podocytes than wild-type cells had migrated into the wound.

FIG 3 CD2AP affects actin dynamics at the cell periphery. Actin dynamics were measured by FRAP in wild-type (WT) and CD2AP-deficient (KO) podocytes stably expressing GFP-actin. (A) A 2-μm^2 area adjacent to the plasma membrane was bleached, and fluorescence recovery was measured over 60 s. The recovery of actin in wild-type cells ($n = 48$) was higher and faster than the recovery of CD2AP-deficient cells ($n = 49$). (B) Nonlinear fit analysis using PRISM5 of FRAP experiments of the periphery of CD2AP WT and CD2AP-deficient podocytes using the average of multiple cells as described for panel A. The half-life of actin recovery in wild-type podocytes is 18.1 ± 0.8 s, and the half-life of actin recovery in CD2AP-deficient podocytes is 39.1 ± 5.5 s. (C) A 2-μm^2 area in the cytoplasm adjacent to the nucleus was bleached, and fluorescence recovery was measured over 30 s. Both wild-type ($n = 6$) and CD2AP-deficient cells ($n = 16$) showed similar rates of recovery.

hibited a patchy and irregular pattern of actin (see Movies S1 and S2 in the supplemental material). These results confirm that CD2AP is important for the structure and dynamics of the actin cytoskeleton at the edge of the cell during spreading.

CD2AP-deficient podocytes have a motility defect. Alterations in the actin-based protrusive structures at the cell edge might be expected to have effects on cell migration. We assessed the role of CD2AP in cell migration using a standard scratch-wound healing assay. Wild-type or CD2AP-deficient podocytes were plated on tissue culture dishes (data not shown) or on glass coverslips (Fig. 2) and allowed to grow to confluence and then differentiated for 2 weeks. A scratch wound was created on the monolayer using a pipette tip, and the cells were monitored for 16 to 24 h by video microscopy. While wild-type cells closed the wound in 14 to 18 h, loss of CD2AP led to slower migration of cells into the wound based on measurements of the thickness of the wound (Fig. 2C) and the number of cells migrated into the wound (Fig. 2D). Video microscopy also demonstrated that while the wild-type podocytes
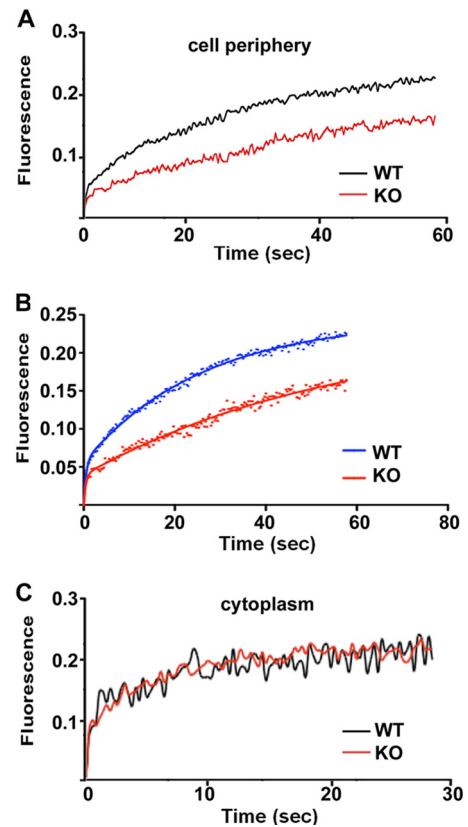
moved in a coordinated sheet-like manner, the CD2AP-deficient podocytes moved more discordantly (see Movies S3 and S4 in the supplemental material). We confirmed that the phenotype was specific to CD2AP and not a clone-specific difference by using two different lentivirus-expressed shRNAs to downregulate CD2AP expression in wild-type cells (data not shown). The shRNA-treated cells behaved similarly to the CD2AP-deficient podocytes, suggesting that the CP recruitment defect mediated by CD2AP also affects cell motility.

CD2AP affects the dynamics of actin at the periphery of the cell. If CD2AP is facilitating CP recruitment to the cell periphery, it might be expected that actin dynamics in the absence of CD2AP would be affected at the cell periphery. We addressed this question using FRAP to measure the turnover of actin filaments in wild-type and CD2AP-deficient podocyte cells stably transfected with GFP-actin. We bleached an area at the periphery of the cell and monitored the fluorescence recovery over the following 60 s (Fig. 3A). In wild-type cells, the mobile fraction was 22%, and the half-time for recovery was 18.1 ± 0.8 s ($n = 49$) (Fig. 3B). In CD2AP-
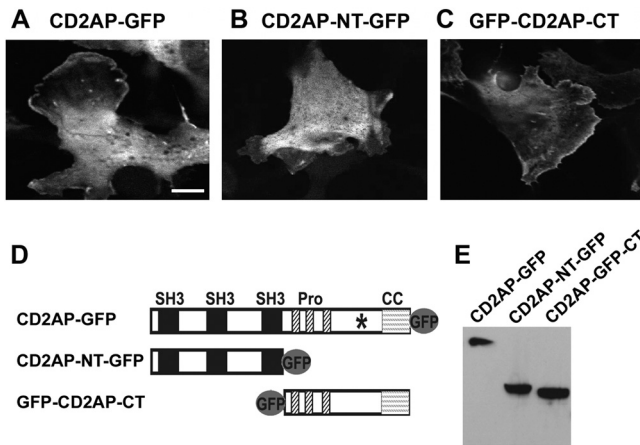
FIG 4 Lamellipodial localization of CD2AP requires its C-terminal domain. (A to C) CD2AP KO podocytes were transfected with cDNAs encoding GFP-tagged full-length CD2AP (GFP-CD2AP), the GFP-tagged N-terminal half of CD2AP (CD2AP-NT), or the GFP-tagged C-terminal half of CD2AP (CD2AP-CT). Twenty-four hours after transfection, cells were replated on glass-bottom dishes and images were acquired using confocal microscopy. Bar, 10 μm. (D) Schematic depiction of GFP-CD2AP constructs. Pro, proline-rich sequence; CC, coiled-coil sequence. The asterisk indicates the binding site for CP. (E) Immunoblotting of CD2AP KO podocytes expressing various GFP-tagged CD2AP constructs.
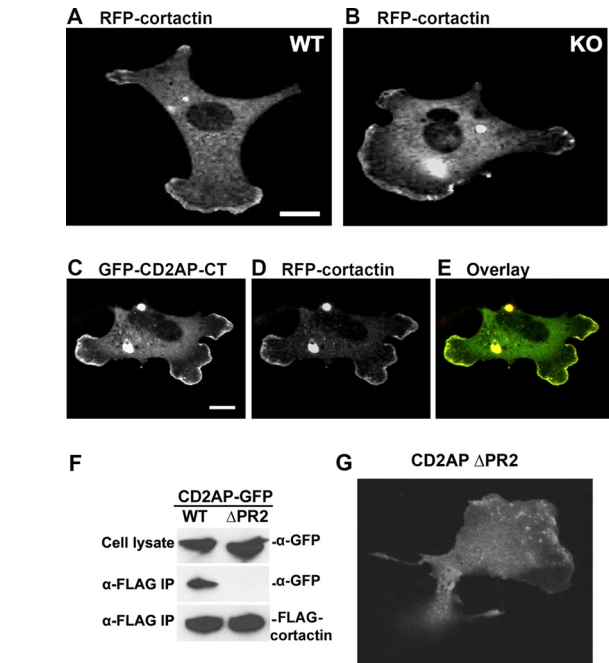

FIG 5 Interaction of CD2AP with cortactin is required for lamellipodial localization. (A and B) Cortactin localization is unaffected by the absence of CD2AP. RFP-cortactin was transfected into wild-type (WT) podocytes (A) or CD2AP-deficient (KO) podocytes (B). Twenty-four hours after transfection, cells were replated and images were acquired using confocal microscopy. Bar, 10 μm. (C to E) Colocalization of CD2AP-CT and cortactin by immunofluorescence microscopy. CD2AP KO podocytes were cotransfected with GFP-CD2AP-CT and RFP-cortactin and imaged as described above. Bar, 10 μm. In the overlay image, CD2AP is green and cortactin is red. (F) CD2AP ΔPR2 mutant does not bind to cortactin. 293T cells were cotransfected with FLAG-cortactin and either the wild type or the ΔPR2 mutant of CD2AP. Cell lysates were prepared and anti-FLAG immunoprecipitates (IP) were immunoblotted with antibodies to FLAG (bottom row) or GFP (top and middle rows). (G) Recruitment of CD2AP to lamellipodia requires the PR2 domain of CD2AP. KO podocytes were transfected with GFP-tagged CD2AP-ΔPR2 and imaged as described above. No significant membrane localization was seen.

deficient cells, the mobile fraction was 16%, and the half-time for recovery was 39.1 ± 5.5 s (n = 49). We also bleached an area in the center of the cell near the nucleus. Here, we saw no difference between wild-type and CD2AP-deficient cells in terms of mobile fraction or recovery time (Fig. 3C). Thus, CD2AP promotes the dynamic turnover of actin filaments at the periphery of the cell, consistent with a role in actin assembly and actin-based motility.

Localization of CD2AP to the cell periphery requires its C terminus and binding to cortactin. To investigate the mechanism of how CD2AP is recruited to the periphery of the cell, we analyzed the localization of various deletion mutants of CD2AP. CD2AP contains several potential protein interaction domains, including three Src homology 3 (SH3) domains at the amino terminus, a proline-rich region, and a coiled-coil domain at the carboxy-terminal half. We first tested a construct consisting of the N-terminal half of CD2AP, including the three SH3 domains (CD2AP-NT), and a second construct consisting of the C-terminal half of CD2AP, including the proline-rich sequences and the coiled-coil domain (CD2AP-CT). Both were fused to GFP. While the C-terminal half of CD2AP localized to the cell periphery in ~51% of cells in a pattern similar to that of full-length CD2AP (~43%), the construct containing the N-terminal half of CD2AP rarely localized to the periphery (~5%) (Fig. 4A to C). Thus, the C-terminal half of CD2AP is necessary and sufficient for its localization to the cell periphery.

It was previously reported that cortactin can interact with the C-terminal half of CD2AP (9), but the function of this interaction was not determined. Cortactin binds to the Arp2/3 complex and actin filaments and promotes Arp2/3 complex-mediated actin polymerization (11, 12, 24, 25). Cortactin is also important for the assembly of actin-based structures that contribute to cell migration (26). We therefore considered whether cortactin mediates the recruitment of CD2AP to the periphery. We first examined the localization of cortactin in wild-type and CD2AP-deficient podo-

cytes. In cells expressing a red fluorescent protein (RFP)-tagged form of cortactin, RFP-cortactin localization was not affected by the loss of CD2AP (Fig. 5A and B), suggesting that cortactin localization does not depend on CD2AP. Furthermore, coexpressing RFP-cortactin and GFP-CD2AP-CT showed that they colocalized in the periphery of CD2AP-deficient podocytes (Fig. 5C to E).

To determine whether a direct interaction between cortactin and CD2AP is important for localization of CD2AP, we generated a CD2AP mutant unable to bind cortactin. Cortactin binds to the second of three proline-rich sequences (PR2) in CD2AP (9). We therefore generated a CD2AP mutant lacking only the second proline-rich sequence (CD2AP-ΔPR2-GFP), and we confirmed that this mutant is unable to bind cortactin by coimmunoprecipitation (Fig. 5F). Localization studies showed that this mutant localized poorly to the cell periphery (~8%), suggesting that direct binding to cortactin is the mechanism for the peripheral localization of CD2AP (Fig. 5G).

To prove this, we used lentiviruses that coexpressed shRNAs targeting cortactin and GFP-CD2AP-CT (Fig. 6A and B). While GFP-CD2AP-CT localized to the periphery in ~56% of podocytes infected with the control shRNA lentivirus (Fig. 6C), CD2AP lo-
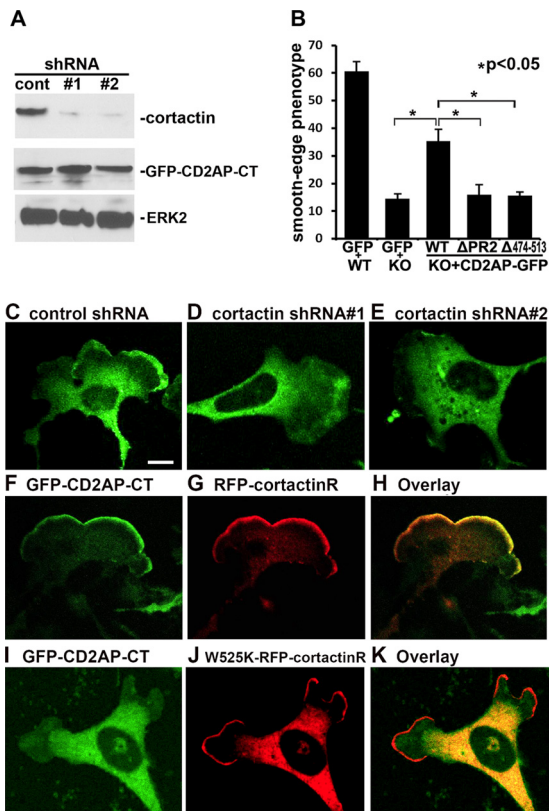
FIG 6 SH3 domain of cortactin is required for CD2AP localization to lamellipodia. (A) Efficient knockdown of cortactin expression using two different shRNA constructs. CD2AP-deficient (KO) podocytes were transduced with lentiviruses coexpressing GFP-CD2AP-CT and a control shRNA (luciferase) or two different cortactin shRNAs (shRNA#1 and shRNA#2). Cell lysates were prepared and immunoblotted with antibodies to cortactin, GFP, or ERK2. (B) CP or cortactin binding mutants of CD2AP are unable to reconstitute the wild-type spreading phenotype. Cell spreading assays of wild-type (WT) podocytes transfected with GFP alone, GFP-WT-CD2AP, or two CD2AP mutants, ΔPR2 and Δ474-513, were evaluated for the spreading morphology after spreading for 15 min. The percentage of cells with the smooth-edge phenotype is shown. (C to E) Recruitment of CD2AP to lamellipodia requires cortactin expression. CD2AP KO podocytes infected with lentiviruses expressing GFP-CD2AP-CT and control or cortactin shRNAs were imaged as described above. Bar, 10 μm. (F to K) Recruitment of CD2AP to lamellipodia requires the SH3 domain of cortactin. A stable cell line from CD2AP-deficient podocytes was generated through transduction with lentiviruses coexpressing an shRNA against cortactin and GFP-CD2AP-CT. The cell lines were transiently transfected with shRNA-resistant forms of either wild-type cortactin (RFP-cortactinR) or an SH3 mutated form of cortactin (W525K-RFP-cortactinR) and were imaged as described above.

calization to the periphery was significantly impaired in CD2AP-deficient podocytes infected with either of two different cortactin shRNA lentiviruses (~11%) (Fig. 6D and E). Since the SH3 domain of cortactin binds directly to CD2AP (9), we next tested whether a cortactin SH3 mutant could rescue the localization of CD2AP. CD2AP-deficient podocytes stably transduced with lentiviruses coexpressing an shRNA against cortactin and GFP-CD2AP-CT were subsequently transfected with plasmids encoding shRNA-resistant forms of either wild-type cortactin (RFP-cortactinR) or an SH3-mutated form of cortactin (W525K-RFP-cortactinR) (15). While wild-type cortactin rescued the peripheral localization of CD2AP (~41%) (Fig. 6F to H), the SH3 mutant could not (~9%) (Fig. 6I to

K). Thus, CD2AP recruitment to the cell periphery requires the SH3 domain of cortactin as well as the second proline-rich motif of CD2AP, most likely via a direct interaction of those regions of the proteins.

To confirm whether cortactin and CP binding to CD2AP was required for lamellipodial function during cell spreading, we reconstituted CD2AP-deficient cells with the cortactin binding mutant (ΔPR2) and the CP binding mutant (Δ474-513) of CD2AP and assessed the morphology of spreading. While the spreading defect was partially rescued by wild-type CD2AP, neither of the two CD2AP mutants, ΔPR2 and Δ474-513, were able to rescue the lamellipodial defect (Fig. 6B). These results demonstrate that interactions with both cortactin and CP are necessary for CD2AP function at the cell periphery during spreading.

CD2AP facilitates cortactin/CP complexes in lamellipodia. Since lamellipodia contain a wide variety of actin-associated proteins (27–29), traditional immunofluorescence colocalization approaches cannot definitively address whether CD2AP/cortactin/CP complexes are present in the cell periphery. We therefore used superresolution fluorescence imaging to determine whether we could detect these complexes at the cell periphery. Superresolution imaging allows for subdiffraction-limit imaging of cellular macromolecular complexes (30–32). We used a stochastic optical reconstruction microscopy (STORM)/photoactivable localization microscopy (PALM) approach, which achieves nanometer-scale resolution of individual molecules inside the cell by repeatedly imaging a sparse subset of single molecules and using photoswitchable probes (18). We hypothesized that if CD2AP functions to link cortactin with CP, the colocalization between the molecules would be higher in the wild type (Fig. 7A and B) than in cells deficient in CD2AP (Fig. 7C and D).

Two-color STORM was used to correlate the positions of cortactin and GFP-CP at the cell periphery in cells (Fig. 7A to D). Since signaling induces CD2AP/cortactin complexes (33), we reasoned that complexes should be enriched at the periphery of the cell compared to the center of the cell. Cortactin/CP colocalization was quantitated using the Manders' colocalization coefficient (Fig. 7E) as well as a pair-correlation algorithm (Fig. 7F) that determines the probability that a second molecule is found within a defined distance from the reference molecule. Both analyses showed that at the cell periphery there was significantly greater colocalization of GFP-CP with cortactin in wild-type (Fig. 7A) compared to CD2AP-deficient cells. In addition, coclustering of CP with cortactin was much lower in the center of the cell. In separate experiments, STORM imaging confirmed that CD2AP colocalizes with CP and cortactin at the periphery of wild-type cells (data not shown). Interestingly, the density of cortactin recruitment was higher in wild-type cells than in CD2AP-deficient cells (Fig. 7A and B versus C and D), suggesting that CD2AP/CP recruitment also functions to further enhance cortactin recruitment (data not shown). This supports our model that CD2AP physically and functionally links CP and cortactin during lamellipodium formation.

DISCUSSION

Previously, we showed that CD2AP interacts with CP (1). Since CP is involved in actin assembly at the plasma membrane (34, 35), we asked here whether CD2AP affected actin assembly and dynamics at the plasma membrane. Supporting an important role for CD2AP in CP function, we found that the recruitment of CP to
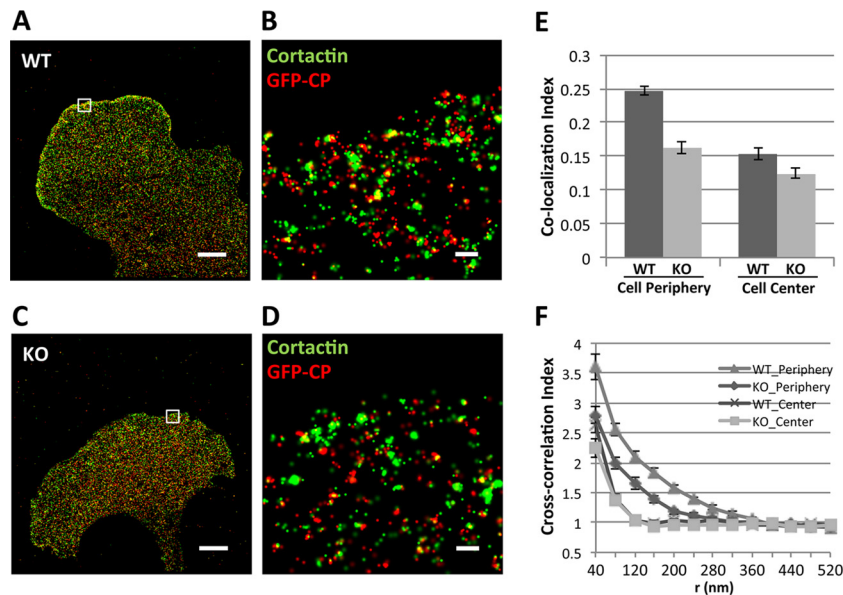
FIG 7 Cortactin and CP complexes at the lamellipodia are facilitated by CD2AP. (A to D) Two-color STORM images of GFP-CP (green) and cortactin (red) were acquired as described in Materials and Methods for wild-type (WT) (A and B) and CD2AP knockout (KO) (C and D) podocytes. Bar, 5 μm. (B and D) A region of the lamellipodia, boxed in panels A and C, is shown at a resolution high enough to allow the position of individual proteins to be determined and the correlation analysis to be performed. Bar, 200 nm. (E) Efficient colocalization of CP with cortactin requires CD2AP. Colocalization analysis of CP and cortactin at the cell periphery in wild-type versus CD2AP knockout cells (left bars) compared to a random position in the cytoplasm (right bars) was first normalized to the density of cortactin and then analyzed using the Manders' overlap coefficient. Analysis was performed on 6 randomly selected cells and 10 regions in each cell. Error bars represent standard deviations. (F) Cross-correlation analysis of CP and cortactin in wild-type versus CD2AP cells was performed on areas of the cell periphery compared to the cytoplasm, with two different secondary antibodies as a negative control. Each point represents the probability that a spot in the second channel is present within a distance of *r* of the spot in the first channel. Values of 1 (*y* axis) are indicative of a random distribution, while values greater than 1 indicate colocalization. Data were acquired and analyzed as described in Materials and Methods.

the cell periphery was defective in CD2AP-deficient cells, and this correlated with defects in cell spreading and cell motility. This effect was specific for the CD2AP-CP interaction, in that expressing a mutated form of CD2AP unable to bind to CP in CD2AP-deficient cells did not rescue the phenotypes. Thus, one important function of CD2AP appears to be the recruitment of CP to the cell periphery.

CP plays a critical role in the ability of cells to form the highly branched actin filament network characteristic of lamellipodia; inhibition of CP at barbed ends, for example, by proteins such as formins and Ena/VASP proteins (23, 36, 37) prevents lamellipodium formation, resulting instead in the assembly of the straight unbranched filaments that support the formation of filopodia (21). By binding to the fast-growing barbed ends at the periphery of the cell, CP is thought to promote the production of short actin filaments and encourage the formation of new branched filaments nucleated by the Arp2/3 complex (12, 34, 38). The switch between filopodia and lamellipodia has been proposed to depend on the local activity of CP (21).

Because of the ability of CP to stop growth at the fast-growing barbed end of actin filaments, CP was originally considered a negative regulator of actin polymerization (35, 39). Indeed, acute inhibition of CP in a small region of the cell leads to a local increase in actin polymerization. However, greater complexity was revealed in other studies. First, analysis of actin assembly and motility in a synthetic Arp2/3 complex-based system revealed that actin-based motility depended on CP concentration in a complex manner, with a bell-shaped curve for motility versus CP concentration. High and low CP concentrations did not support Arp2/3

complex-mediated actin assembly and motility as well as an optimal middle concentration did (40). Second, long-term knockdown of CP in cultured cells resulted in decreased lamellipodia, which appeared to result from decreased Arp2/3 complex-mediated actin polymerization (21). One potential molecular explanation for this result is that the level of CP controls the length of actin filament branches in the network and that networks require optimal branch lengths in order to support the force produced by growing actin filament ends as they push outward on the plasma membrane.

One outstanding question is to what extent CD2AP inhibits the actin capping activity of CP. We previously showed that CD2AP can inhibit the actin capping activity of CP, but the effect is partial and not complete (1). Consistent with this, structural studies demonstrate that the CP-binding motif found in CD2AP binds at a site distinct from the actin-binding surface (1, 8), suggesting that CP bound to CD2AP still retains actin capping activity. For these reasons, we speculate that the CP that is targeted to the cell periphery by CD2AP is not inhibited and caps barbed ends.

CD2AP has a particularly critical role in the podocyte, as revealed by the significant kidney phenotype that develops in the CD2AP-knockout mouse (4). CD2AP has an ortholog, CIN85, that retains the CP binding site and may be able to function in place of CD2AP (41). Podocytes, however, express CD2AP but not CIN85 (41), so the absence of both proteins may be required to produce the phenotypes seen here. Indeed, the migration and the spreading defects that we observed were not apparent in CD2AP-deficient mouse embryonic fibroblasts that express CIN85 (data not shown). Because the ability of podocytes to

spread and cover exposed areas of the glomerular basement membrane may be an important response to kidney injury, the defect in CP recruitment and lamellipodia formation described here may explain the kidney failure that develops in the CD2AP-deficient mice (4).

Our finding that cortactin can recruit CD2AP, which then recruits CP, provides novel insight into the mechanism of actin polymerization at the cell periphery. Cortactin was first discovered as a major substrate for the Src tyrosine kinase (42). Cortactin contains an acidic Arp2/3 complex-binding region at the N terminus, similar to regions in WASP and the SCAR/WAVE proteins, followed by an F-actin-binding region and an SH3 domain at the C terminus. The SH3 domain is able to bind proline-rich sequences in a variety of proteins, including CD2AP, WASP, WIP, Shank2, dynamin 2, and Fgd1 (9, 10, 43–45). By coupling modifiers of actin polymerization via its SH3 domain, cortactin may function to generate different types of actin structures in the cell.

Cortactin is known to enhance actin polymerization in lamellipodia through its ability to promote the formation of and stabilize Arp2/3 complex-based branched actin filaments (11, 26). Cortactin is recruited to lamellipodia via its N-terminal and F-actin-binding regions, suggesting that the Arp2/3 complex and actin filaments assembled at the cell periphery during spreading are responsible for cortactin recruitment (42, 46). Our data showing that cortactin then recruits CD2AP and CP demonstrate how it uses its SH3 domain of cortactin to specifically enhance and sustain branched actin fiber assembly in lamellipodia. By recruiting CP, CD2AP may generate a positive-feedback loop, with increased branched actin filaments allowing for the recruitment of additional cortactin molecules. This could explain the decreased density of peripheral cortactin in CD2AP-deficient cells (data not shown). Thus, CD2AP synergizes the capping of fast-growing barbed ends by CP with the Arp2/3 complex-based branching activity of cortactin. Supporting this idea is the fact that growth factor stimulation of lamellipodium formation is known to induce cortactin/CD2AP complexes (33).

Protein-protein interactions are easily detected using biochemical approaches, but verifying their existence in cells remains a significant challenge. While two-color immunofluorescence colocalization studies are often employed to support a specific interaction, these studies are limited by the low resolution of light microscopic imaging and often the very broad cellular expression patterns of a specific protein. Electron microscopy with immunogold labeling can overcome some of the resolution issues, but this method is highly cumbersome and the number of proteins labeled is often highly limited. One utility of superresolution methods like STORM and PALM (32, 47) is that they can robustly localize thousands of single molecules at nanometer resolution and allow for rigorous statistical analytic tools to be applied to the problem of colocalization (48). Using two analytic approaches, a colocalization and a cross-correlation analysis, we could easily show that the colocalization of CP and cortactin at the cell periphery required the presence of CD2AP, a conclusion that was not apparent by visual inspection of the images. We believe that the quantitative analysis of protein interactions using STORM and/or PALM will be especially powerful to validate protein-protein interactions that are of low stoichiometry and occur at specific locations in the cell.

In summary, we have demonstrated that two proteins, CP and cortactin, previously known to be important for actin assembly and cell migration, form a complex with CD2AP at the periphery of the cell. By binding cortactin, CD2AP functions to recruit CP to the periphery of spreading cells. CD2AP thus plays a critical scaffolding role to enhance the ability of CP and cortactin to promote Arp2/3 complex-mediated actin assembly. Branched actin filaments are also important in vesicular trafficking and endocytosis, so these findings provide insight into other possible roles for CD2AP in the function of normal and diseased cells and tissues.

REFERENCES

1. Bruck S, Huber TB, Ingham RJ, Kim K, Niederstrasser H, Allen PM, Pawson T, Cooper JA, Shaw AS. 2006. Identification of a novel inhibitory actin-capping protein binding motif in CD2-associated protein. J. Biol. Chem. 281:19196–19203.

2. Dustin ML, Olszowy MW, Holdorf AD, Li J, Bromley S, Desai N, Widder P, Rosenberger F, van der Merwe PA, Allen PM, Shaw AS. 1998. A novel adaptor protein orchestrates receptor patterning and cytoskeletal polarity in T-cell contacts. Cell 94:667–677.

3. Li C, Ruotsalainen V, Tryggvason K, Shaw AS, Miner JH. 2000. CD2AP is expressed with nephrin in developing podocytes and is found widely in mature kidney and elsewhere. Am. J. Physiol. Renal Physiol. 279:F785–F792.

4. Shih NY, Li J, Karpitskii V, Nguyen A, Dustin ML, Kanagawa O, Miner JH, Shaw AS. 1999. Congenital nephrotic syndrome in mice lacking CD2-associated protein. Science 286:312–315.

5. Hollingworth P, Harold D, Sims R, Gerrish A, Lambert JC, Carrasquillo MM, Abraham R, Hamshere ML, Pahwa JS, Moskvina V, Dowzell K, Jones N, Stretton A, Thomas C, Richards A, Ivanov D, Widdowson C, Chapman J, Lovestone S, Powell J, Proitsi P, Lupton MK, Brayne C, Rubinsztein DC, Gill M, Lawlor B, Lynch A, Brown KS, Passmore PA, Craig D, McGuinness B, Todd S, Holmes C, Mann D, Smith AD, Beaumont H, Warden D, Wilcock G, Love S, Kehoe PG, Hooper NM, Vardy ER, Hardy J, Mead S, Fox NC, Rossor M, Collinge J, Maier W, Jessen F, Ruther E, Schurmann B, Heun R, Kolsch H, van den Bussche H, Heuser I, Kornhuber J, Wiltfang J, Dichgans M, Frolich L, Hampel H, Gallacher J, Hull M, Rujescu D, Giegling I, Goate AM, Kauwe JS, Cruchaga C, Nowotny P, Morris JC, Mayo K, Sleegers K, Bettens K, Engelborghs S, De Deyn PP, Van Broeckhoven C, Livingston G, Bass NJ, Gurling H, McQuillin A, Gwilliam R, Deloukas P, AL-Chalabi A, Shaw CE, Tsolaki M, Singleton AB, Guerreiro R, Muhleisen TW, Nothen MM, Moebus S, Jockel KH, Klopp N, Wichmann HE, Pankratz VS, Sando SB, Aasly JO, Barcikowska M, Wszolek ZK, Dickson DW, Graff-Radford NR, Petersen RC, Alzheimer'S Disease Neuroimaging Initiative, van Duijn CM, Breteler MM, Ikram MA, DeStefano AL, Fitzpatrick AL, Lopez O, Launer LJ, Seshadri S; CHARGE Consortium, Berr C, Campion D, Epelbaum J, Dartigues JF, Tzourio C, Alpérovitch A, Lathrop M, EADI1 Consortium, Feulner TM, Friedrich P, Riehle C, Krawczak M, Schreiber S, Mayhaus M, Nicolhaus S, Wagenpfeil S, Steinberg S, Stefansson H, Stefansson K, Snaedal J, Björnsson S, Jonsson PV, Chouraki V, Genier-Boley B, Hiltunen M, Soininen H, Combarros O, Zelenika D, Delepine M, Bullido MJ, Pasquier F, Mateo I, Frank-Garcia A, Porcellini E, Hanon O, Coto E, Alvarez V, Bosco P, Siciliano G, Mancuso M, Panza F, Solfrizzi V, Nacmias B, Sorbi S, Bossù P, Piccardi P, Arosio B, Annoni G, Seripa D, Pilotto A, Scarpini E, Galimberti D, Brice A, Hannequin D, Licastro F, Jones L, Holmans PA, Jonsson T, Riemenschneider M, Morgan K, Younkin SG, Owen MJ, O'Donovan M, Amouyel P, Williams J. 2011. Common variants at ABCA7, MS4A6A/MS4A4E, EPHA1, CD33 and CD2AP are associated with Alzheimer's disease. Nat. Genet. 43:429–435.

6. Naj AC, Jun G, Beecham GW, Wang LS, Vardarajan BN, Buros J, Gallins PJ, Buxbaum JD, Jarvik GP, Crane PK, Larson EB, Bird TD,

Boeve BF, Graff-Radford NR, De Jager PL, Evans D, Schneider JA, Carrasquillo MM, Ertekin-Taner N, Younkin SG, Cruchaga C, Kauwe JS, Nowotny P, Kramer P, Hardy J, Huentelman MJ, Myers AJ, Barmada MM, Demirci FY, Baldwin CT, Green RC, Rogaeva E, ST. George-Hyslop P, Arnold SE, Barber R, Beach T, Bigio EH, Bowen JD, Boxer A, Burke JR, Cairns NJ, Carlson CS, Carney RM, Carroll SL, Chui HC, Clark DG, Corneveaux J, Cotman CW, Cummings JL, DeCarli C, DeKosky ST, Diaz-Arrastia R, Dick M, Dickson DW, Ellis WG, Faber KM, Fallon KB, Farlow MR, Ferris S, Frosch MP, Galasko DR, Ganguli M, Gearing M, Geschwind DH, Ghetti B, Gilbert JR, Gilman S, Giordani B, Glass JD, Growdon JH, Hamilton RL, Harrell LE, Head E, Honig LS, Hulette CM, Hyman BT, Jicha GA, Jin LW, Johnson N, Karlawish J, Karydas A, Kaye JA, Kim R, Koo EH, Kowall NW, Lah JJ, Levey AI, Lieberman AP, Lopez OL, Mack WJ, Marson DC, Martiniuk F, Mash DC, Masliah E, McCormick WC, McCurry SM, McDavid AN, McKee AC, Mesulam M, Miller BL, Miller CA, Miller JW, Parisi JE, Perl DP, Peskind E, Petersen RC, Poon WW, Quinn JF, Rajbhandary RA, Raskind M, Reisberg B, Ringman JM, Roberson ED, Rosenberg RN, Sano M, Schneider LS, Seeley W, Shelanski ML, Slifer MA, Smith CD, Sonnen JA, Spina S, Stern RA, Tanzi RE, Trojanowski JQ, Troncoso JC, Van Deerlin VM, Vinters HV, Vonsattel JP, Weintraub S, Welsh-Bohmer KA, Williamson J, Woltjer RL, Cantwell LB, Dombroski BA, Beekly D, Lunetta KL, Martin ER, Kamboh MI, Saykin AJ, Reiman EM, Bennett DA, Morris JC, Montine TJ, Goate AM, Blacker D, Tsuang DW, Hakonarson H, Kukull WA, Foroud TM, Haines JL, Mayeux R, Pericak-Vance MA, Farrer LA, Schellenberg GD. 2011. Common variants at MS4A4/MS4A6E, CD2AP, CD33 and EPHA1 are associated with late-onset Alzheimer's disease. Nat. Genet. **43**:436–441.

7. **Hutchings NJ, Clarkson N, Chalkley R, Barclay AN, Brown MH.** 2003. Linking the T cell surface protein CD2 to the actin-capping protein CAPZ via CMS and CIN85. J. Biol. Chem. **278**:22396–22403.

8. **Hernandez-Valladares M, Kim T, Kannan B, Tung A, Aguda AH, Larsson M, Cooper JA, Robinson RC.** 2010. Structural characterization of a capping protein interaction motif defines a family of actin filament regulators. Nat. Struct. Mol. Biol. **17**:497–503.

9. **Lynch DK, Winata SC, Lyons RJ, Hughes WE, Lehrbach GM, Wasinger V, Corthals G, Cordwell S, Daly RJ.** 2003. A cortactin-CD2-associated protein (CD2AP) complex provides a novel link between epidermal growth factor receptor endocytosis and the actin cytoskeleton. J. Biol. Chem. **278**:21805–21813.

10. **Kinley AW, Weed SA, Weaver AM, Karginov AV, Bissonette E, Cooper JA, Parsons JT.** 2003. Cortactin interacts with WIP in regulating Arp2/3 activation and membrane protrusion. Curr. Biol. **13**:384–393.

11. **Weaver AM, Heuser JE, Karginov AV, Lee WL, Parsons JT, Cooper JA.** 2002. Interaction of cortactin and N-WASp with Arp2/3 complex. Curr. Biol. **12**:1270–1278.

12. **Weed SA, Karginov AV, Schafer DA, Weaver AM, Kinley AW, Cooper JA, Parsons JT.** 2000. Cortactin localization to sites of actin assembly in lamellipodia requires interactions with F-actin and the Arp2/3 complex. J. Cell Biol. **151**:29–40.

13. **Nosaka T, Kawashima T, Misawa K, Ikuta K, Mui AL, Kitamura T.** 1999. STAT5 as a molecular regulator of proliferation, differentiation and apoptosis in hematopoietic cells. EMBO J. **18**:4754–4765.

14. **Feng Y, Nie L, Thakur MD, Su Q, Chi Z, Zhao Y, Longmore GD.** 2010. A multifunctional lentiviral-based gene knockdown with concurrent rescue that controls for off-target effects of RNAi. Genomics Proteomics Bioinformatics **8**:238–245.

15. **Tehrani S, Faccio R, Chandrasekar I, Ross FP, Cooper JA.** 2006. Cortactin has an essential and specific role in osteoclast actin assembly. Mol. Biol. Cell **17**:2882–2895.

16. **Shih NY, Li J, Cotran R, Mundel P, Miner JH, Shaw AS.** 2001. CD2AP localizes to the slit diaphragm and binds to nephrin via a novel C-terminal domain. Am. J. Pathol. **159**:2303–2308.

17. **Morita S, Kojima T, Kitamura T.** 2000. Plat-E: an efficient and stable system for transient packaging of retroviruses. Gene Ther. **7**:1063–1066.

18. **Dani A, Huang B, Bergan J, Dulac C, Zhuang X.** 2010. Superresolution imaging of chemical synapses in the brain. Neuron **68**:843–856.

19. **Sengupta P, Jovanovic-Talisman T, Skoko D, Renz M, Veatch SL, Lippincott-Schwartz J.** 2011. Probing protein heterogeneity in the plasma membrane using PALM and pair correlation analysis. Nat. Methods **8**:969–975.

20. **Manders EM, Hoebe R, Strackee J, Vossepoel AM, Aten JA.** 1996. Largest contour segmentation: a tool for the localization of spots in confocal images. Cytometry **23**:15–21.

21. **Mejillano MR, Kojima S, Applewhite DA, Gertler FB, Svitkina TM, Borisy GG.** 2004. Lamellipodial versus filopodial mode of the actin nanomachinery: pivotal role of the filament barbed end. Cell **118**:363–373.

22. **Vitriol EA, Uetrecht AC, Shen F, Jacobson K, Bear JE.** 2007. Enhanced EGFP-chromophore-assisted laser inactivation using deficient cells rescued with functional EGFP-fusion proteins. Proc. Natl. Acad. Sci. U. S. A. **104**:6702–6707.

23. **Applewhite DA, Barzik M, Kojima S, Svitkina TM, Gertler FB, Borisy GG.** 2007. Ena/VASP proteins have an anti-capping independent function in filopodia formation. Mol. Biol. Cell **18**:2579–2591.

24. **Uruno T, Liu J, Zhang P, Fan Y, Egile C, Li R, Mueller SC, Zhan X.** 2001. Activation of Arp2/3 complex-mediated actin polymerization by cortactin. Nat. Cell Biol. **3**:259–266.

25. **Wu C, Asokan SB, Berginski ME, Haynes EM, Sharpless NE, Griffith JD, Gomez SM, Bear JE.** 2012. Arp2/3 is critical for lamellipodia and response to extracellular matrix cues but is dispensable for chemotaxis. Cell **148**:973–987.

26. **Ammer AG, Weed SA.** 2008. Cortactin branches out: roles in regulating protrusive actin dynamics. Cell Motil. Cytoskeleton **65**:687–707.

27. **Small JV.** 1994. Lamellipodia architecture: actin filament turnover and the lateral flow of actin filaments during motility. Semin. Cell Biol. **5**:157–163.

28. **Small JV, Auinger S, Nemethova M, Koestler S, Goldie KN, Hoenger A, Resch GP.** 2008. Unravelling the structure of the lamellipodium. J. Microsc. **231**:479–485.

29. **Small JV, Stradal T, Vignal E, Rottner K.** 2002. The lamellipodium: where motility begins. Trends Cell Biol. **12**:112–120.

30. **Betzig E, Patterson GH, Sougrat R, Lindwasser OW, Olenych S, Bonifacino JS, Davidson MW, Lippincott-Schwartz J, Hess HF.** 2006. Imaging intracellular fluorescent proteins at nanometer resolution. Science **313**:1642–1645.

31. **Hell SW.** 2009. Microscopy and its focal switch. Nat. Methods **6**:24–32.

32. **Huang B, Bates M, Zhuang X.** 2009. Super-resolution fluorescence microscopy. Annu. Rev. Biochem. **78**:993–1016.

33. **Bryce NS, Clark ES, Leysath JL, Currie JD, Webb DJ, Weaver AM.** 2005. Cortactin promotes cell motility by enhancing lamellipodial persistence. Curr. Biol. **15**:1276–1285.

34. **Schafer DA, Jennings PB, Cooper JA.** 1996. Dynamics of capping protein and actin assembly in vitro: uncapping barbed ends by polyphosphoinositides. J. Cell Biol. **135**:169–179.

35. **Wear MA, Yamashita A, Kim K, Maeda Y, Cooper JA.** 2003. How capping protein binds the barbed end of the actin filament. Curr. Biol. **13**:1531–1537.

36. **Barzik M, Kotova TI, Higgs HN, Hazelwood L, Hanein D, Gertler FB, Schafer DA.** 2005. Ena/VASP proteins enhance actin polymerization in the presence of barbed end capping proteins. J. Biol. Chem. **280**:28653–28662.

37. **Bear JE, Svitkina TM, Krause M, Schafer DA, Loureiro JJ, Strasser GA, Maly IV, Chaga OY, Cooper JA, Borisy GG, Gertler FB.** 2002. Antagonism between Ena/VASP proteins and actin filament capping regulates fibroblast motility. Cell **109**:509–521.

38. **Akin O, Mullins RD.** 2008. Capping protein increases the rate of actin-based motility by promoting filament nucleation by the Arp2/3 complex. Cell **133**:841–851.

39. **Cooper JA, Pollard TD.** 1985. Effect of capping protein on the kinetics of actin polymerization. Biochemistry **24**:793–799.

40. **Loisel TP, Boujemaa R, Pantaloni D, Carlier MF.** 1999. Reconstitution of actin-based motility of Listeria and Shigella using pure proteins. Nature **401**:613–616.

41. **Grunkemeyer JA, Kwoh C, Huber TB, Shaw AS.** 2005. CD2-associated protein (CD2AP) expression in podocytes rescues lethality of CD2AP deficiency. J. Biol. Chem. **280**:29677–29681.

42. **Wu H, Parsons JT.** 1993. Cortactin, an 80/85-kilodalton pp60src substrate, is a filamentous actin-binding protein enriched in the cell cortex. J. Cell Biol. **120**:1417–1426.

43. **Du Y, Weed SA, Xiong WC, Marshall TD, Parsons JT.** 1998. Identification of a novel cortactin SH3 domain-binding protein and its localization to growth cones of cultured neurons. Mol. Cell. Biol. **18**:5838–5851.

44. **Hou P, Estrada L, Kinley AW, Parsons JT, Vojtek AB, Gorski JL.** 2003. Fgd1, the Cdc42 GEF responsible for faciogenital dysplasia, directly inter-

acts with cortactin and mAbp1 to modulate cell shape. Hum. Mol. Genet. **12**:1981–1993.

45. **Schafer DA, Weed SA, Binns D, Karginov AV, Parsons JT, Cooper JA.** 2002. Dynamin2 and cortactin regulate actin assembly and filament organization. Curr. Biol. **12**:1852–1857.

46. **Weed SA, Parsons JT.** 2001. Cortactin: coupling membrane dynamics to cortical actin assembly. Oncogene **20**:6418–6434.

47. **Bates M, Huang B, Dempsey GT, Zhuang X.** 2007. Multicolor super-resolution imaging with photo-switchable fluorescent probes. Science **317**:1749–1753.

48. **Sherman E, Barr V, Manley S, Patterson G, Balagopalan L, Akpan I, Regan CK, Merrill RK, Sommers CL, Lippincott-Schwartz J, Samelson LE.** 2011. Functional nanoscale organization of signaling molecules downstream of the T cell antigen receptor. Immunity **35**:705–720.